

Highlights

Isolating the mechanisms for asteroid surface refreshing

Francesca E. DeMeo, Michaël Marset, David Polishook, Brian J. Burt, Richard P. Binzel, Sunao Hasegawa, Mikael Granvik, Nicholas A. Moskovitz, Alissa Earle, Schelte J. Bus, Cristina A. Thomas, Andrew S. Rivkin, Stephen M. Slivan

- We analyze visible and near-ir spectra of 477 S-complex NEOs and Mars Crossers
- We calculate the fresh-to-space-weathered (Q/S) ratio to understand physical processes
- The Q/S ratio depends on size, perihelion, inclination, and MOID.
- No single resurfacing mechanism can explain all of these trends
- Four mechanisms are likely: YORP, thermal degradation, planetary encounters, and collisions.

Isolating the mechanisms for asteroid surface refreshing

Francesca E. DeMeo^{a,*}, Michaël Marsset^{a,b}, David Polishook^c, Brian J. Burt^{a,d}, Richard P. Binzel^a, Sunao Hasegawa^e, Mikael Granvik^{f,g}, Nicholas A. Moskovitz^d, Alissa Earle^a, Schelte J. Bus^h, Cristina A. Thomasⁱ, Andrew S. Rivkin^j and Stephen M. Slivan^a

^aDepartment of Earth, Atmospheric, and Planetary Sciences, Massachusetts Institute of Technology, 77 Massachusetts Avenue, Cambridge, MA 02139 USA

^bEuropean Southern Observatory (ESO), Alonso de Cordova 3107, 1900 Casilla Vitacura, Santiago, Chile

^cFaculty of Physics, Weizmann Institute of Science, Rehovot 0076100, Israel

^dLowell Observatory, 1400 West Mars Hill Road, Flagstaff, AZ 86001, USA

^eInstitute of Space and Astronautical Science, Japan Aerospace Exploration Agency, 3-1-1 Yoshinodai, Chuo-ku, Sagami-hara, Kanagawa 252-5210, Japan

^fDepartment of Physics, University of Helsinki, PO Box 64, FI-00014 Helsinki, Finland

^gAsteroid Engineering Lab, Space Systems, Luleå University of Technology, Box 848, S-98128 Kiruna, Sweden

^hInstitute for Astronomy, University of Hawaii, 2860 Woodlawn Drive, Honolulu, HI 96822-1839, USA

ⁱNorthern Arizona University, Department of Astronomy and Planetary Science PO Box 6010, Flagstaff, AZ 86011 USA

^jThe Johns Hopkins University Applied Physics Laboratory, Laurel, MD, USA

ARTICLE INFO

Keywords:

Asteroids
Asteroids, surfaces
Near-Earth objects,
Spectroscopy

ABSTRACT

Evidence is seen for young, fresh surfaces among Near-Earth and Main-Belt asteroids even though space-weathering timescales are shorter than the age of the surfaces. A number of mechanisms have been proposed to refresh asteroid surfaces on short timescales, such as planetary encounters, YORP spinup, thermal degradation, and collisions. Additionally, other factors such as grain size effects have been proposed to explain the existence of these “fresh-looking” spectra. To investigate the role each of these mechanisms may play, we collected a sample of visible and near-infrared spectra of 477 near-Earth and Mars Crosser asteroids with similar sizes and compositions - all with absolute magnitude $H > 16$ and within the S-complex and having olivine to pyroxene (ol/(ol+opx)) ratios > 0.65 . We taxonomically classify these objects in the Q (fresh) and S (weathered) classes. We find four trends in the Q/S ratio: 1) previous work demonstrated the Q/S ratio increases at smaller sizes down to $H \lesssim 16$, but we find a sharp increase near $H \sim 19$ after which the ratio decreases monotonically. 2) in agreement with many previous studies, the Q/S ratio increases with decreasing perihelion distance, and we find it is non-zero for larger perihelia $> 1.2\text{AU}$, 3) as a new finding our work reveals the Q/S ratio has a sharp, significant peak near $\sim 5^\circ$ orbital inclination, and 4) we confirm previous findings that the Q/S ratio is higher for objects that have the possibility of encounter with Earth and Venus versus those that don't, however this finding cannot be distinguished from the perihelion trend. No single resurfacing mechanism can explain all of these trends, so multiple mechanisms are required. YORP spin-up scales with size, thermal degradation is dependent on perihelion, planetary encounters trend with inclination, perihelion and MOID, noting that asteroid-asteroid collisions are also dependent on inclination. It is likely that a combination of all four resurfacing mechanisms are needed to account for all observational trends.

1. Introduction

Asteroid spectra reflect both compositional information about the surface as well as non-compositional information. Spectra are dependent on factors such as the grain size of the particles on the asteroid surface, phase angle of the observation, temperature, and by Earth observing conditions of the night such as the airmass (Johnson and Fanale 1973; Hapke 1981; Roush 1984; Hiroi and Pieters 1992; Hapke 1981; Sanchez et al. 2012; Reddy et al. 2015; Vernazza et al. 2016; Marsset et al. 2020).

*Corresponding author, fdemeo@mit.edu

ORCID(s): 0000-0002-8397-4219 (F.E. DeMeo); 0000-0001-8617-2425 (M. Marsset); 0000-0002-6977-3146 (D. Polishook); 0000-0002-6423-0716 (B.J. Burt); 0000-0002-9995-7341 (R.P. Binzel); 0000-0001-6366-2608 (S. Hasegawa); 0000-0002-5624-1888 (M. Granvik); 0000-0001-6765-6336 (N.A. Moskovitz); 0000-0002-2780-7037 (A. Earle); 0000-0003-4191-6536 (S.J. Bus); 0000-0003-3091-5757 (C.A. Thomas); 0000-0002-9939-9976 (A.S. Rivkin); 0000-0003-3291-8708 (S.M. Slivan)

Additionally, asteroids are exposed to the space environment which can physically and chemically alter their surfaces over time. This process is called space weathering, an umbrella term that includes many processes such as bombardment by high energy particles from the sun, cosmic rays, and micrometeorite bombardment (Hapke 1965, 2001). This process was first studied on the moon, confirmed with Apollo samples (e.g. Hapke et al. 1970).

For decades, studies were undertaken to determine the cause of the spectral slope mismatch between many S-complex asteroids and ordinary chondrite meteorites. Lunar-style space weathering was established as playing an important role, reddening the slopes over time, as seen from asteroid spectral studies, laboratory weathering experiments, and ground-truth of sample return from asteroid Itokawa by the JAXA Hayabusa spacecraft (e.g., Binzel et al. 2001b; Hiroi et al. 2006; Brunetto et al. 2006; Nakamura et al. 2011). Different space weathering effects are seen on other asteroid types such as on Vesta (Pieters et al. 2012).

Near Earth Objects (NEOs), Mars Crossers (MCs), and small Main Belt Asteroids (MBAs) often display fresh “unweathered” surfaces with low spectral slopes and deep 1- μ m bands due to olivine and pyroxene, spectrally classified as Q-type asteroids. Because space weathering acts on short timescales (<1 My, Vernazza et al. 2009), one could ask: why would we find any fresh surfaces at all? A number of mechanisms have been proposed to rejuvenate asteroid surfaces.

Planetary Encounters: Numerous studies of the orbital trends of Q-types, particularly perihelion distance and the Minimum Orbit Intersection Distance (MOID, Bonanno 2000) to the terrestrial planets suggested close planetary encounters (within \sim 5-16 planetary radii), particularly with Earth and Venus, are the dominant mechanism for surface refreshing (Nesvorný et al. 2005; Marchi et al. 2006; Binzel et al. 2010; Nesvorný et al. 2010). While Q-types were discovered that encounter only Mars, but not Earth and Venus (DeMeo et al. 2014), it was shown that S-type and Q-type asteroids have similar probabilities of an encounter with Mars, while Q-types statistically have more encounters with Venus and Earth than S-types (Carry et al. 2016). Additionally, while an increase of Q-types was found at low MOIDs for Venus and Earth, no excess was seen for Mars, further emphasizing the negligible role Mars plays in surface refreshing (Devogèle et al. 2019).

YORP spin up: Planetary encounters cannot be the sole explanation for the existence of fresh Q-type surfaces. First, Q-types exist that do not have orbital histories that allow planetary encounters, including among Main Belt Objects. Second, the effects of planetary encounters are not size dependent yet the relative abundance of Q-types increases at smaller sizes (Binzel et al. 2004b; Mothé-Diniz and Nesvorný 2008; Rivkin et al. 2011; Thomas et al. 2011, 2012; Lin et al. 2015; Carry et al. 2016; Graves et al. 2018). Graves et al. (2018) found the change in slope among S-complex asteroids as a function of size was consistent among NEOs, MCs, and MBAs suggesting a common mechanism.

The Yarkovsky–O’Keefe–Radzievskii–Paddack effect (YORP) describes the process where thermal emission from an irregularly-shaped body can produce a torque that changes the spin rate of that object over time, causing the body to spin up or spin down (Rubincam 2000). If the spin rate becomes fast enough, material from the surface moves to the equator or is shed from the body, exposing fresh material and even causing the body to fracture (Walsh et al. 2008; Hirabayashi 2015). Graves et al. (2018) created a resurfacing model from YORP spin-up that could qualitatively explain this decrease in average slope (more Q-type-like) with decreasing size. It could also explain the existence of fresh surfaces at higher perihelia - because the rate of YORP spin-up and space weathering are both dominated by solar radiation there should be no orbital dependence on refresh rates, as discussed in Graves et al. (2018).

Further support for YORP spinup as a resurfacing mechanism comes from observation of young asteroid pairs. A number of observations have been made of young asteroid pairs in the main belt that were formed by rotational fission, meaning the progenitor body’s spin rate was increased by YORP to a point where the body split apart into fragments on similar orbits (Moskovitz 2012; Polishook et al. 2014; Moskovitz et al. 2019). A Q-type asteroid was found among those pairs (Polishook et al. 2014).

Collisions and small impacts: Richardson et al. (2005) modeled the effects of impact-induced seismic activity on asteroid surfaces. They found that small impacts could globally modify the surface including reducing craters. These impacts would also plausibly reset the space weathering age of the surface by exposing fresh material (Shestopalov et al. 2013).

Rivkin et al. (2011) and DeMeo et al. (2014) estimated with rough order-of-magnitude calculations that the timescale of small impacts able to cause seismic activity that globally resets the regolith on small bodies, both among NEOs and MBAs, is compatible with estimates of the timescale of space weathering.

Both YORP and collisions should be more effective at surface refreshing at smaller sizes. However, the effect of YORP is inclination independent, while collisions would be much more effective for NEOs that have lower inclinations and spend a significant portion of their lifetime in the main belt. Dell’Oro et al. (2011) found a correlation between

the degree of space weathering of an NEO and its probability and intensity of collision.

Thermal Degradation: Thermal degradation, also called thermal fatigue or thermally induced surface degradation, is a process by which the diurnal temperature variation on a body breaks up rocks on the surface, and is expected to be the dominant process for regolith creation on small asteroids (Delbo et al. 2014) and even complete disintegration of bodies at low perihelia (Granvik et al. 2016). Larger boulders experience higher stress than smaller ones, and the effect seems minimal for rock sizes below 30 cm (Molaro et al. 2017).

Graves et al. (2019) modeled the resurfacing of asteroids due to close planetary encounters and to thermally induced surface degradation, assuming a power law relationship between the resurfacing timescale and the solar distance for degradation. They find that resurfacing from close encounters cannot reproduce the observed spectral slope trend with perihelion distribution. They also find a much better fit for thermal degradation and suggest that thermal processes are the best explanation for resurfacing asteroids with low perihelia ($q \leq 0.9$ AU).

Cases against resurfacing mechanisms: Mothé-Diniz et al. (2010) found that over visible wavelengths there are ordinary chondrite spectra that match S-complex asteroids that have higher slopes. They suggest that many S-complex asteroids are actually unweathered.

Hapke (2001) suggested that surfaces with less fine regolith (larger grains or boulders) would present a less weathered spectrum. Additionally, Hasegawa et al. (2019) show through laboratory irradiation experiments that for larger-grained ($>100\mu\text{m}$) samples the spectral slopes are neutral, suggesting that Q-type asteroids could be weathered bodies dominated by large grains on the surface. They find that the space weathering timescales are shorter than the timescales for planetary encounters so as much as half of the Q-type population cannot be fully explained by encounters, and suggest some Q-types have large-grained weathered surfaces. Contrary to these findings, Itokawa is covered with regolith on parts of its surface and with boulders on other parts, and both regolith-rich and boulder-rich areas present very similar reflectance spectra (Abe et al. 2006). Regions with little fine regolith were found to be highly weathered (Ishiguro et al. 2007). The relationship between composition, grain size, and space weathering is complex and requires further analysis.

The main scientific objective of this work is to resolve the nature of these most fundamental physical processes that shape the surfaces of the asteroid population. We seek to reduce the spectral effects caused by composition to focus on the effects of space weathering. We use a sample of 477 S-complex NEOs and Mars Crossers with absolute magnitudes (H) greater than 16 and that have high olivine content ($\text{ol}/(\text{ol}+\text{opx}) \geq 0.65$) consistent with L- and LL-chondrites to maintain compositional homogeneity. We explore the fresh-to-weathered (Q/S) ratios of populations of bodies based on their orbital and physical characteristics as well as their orbital history and potential for encounter with planets.

2. Data

We include visible and near-infrared spectra of 477 S-complex NEOs and Mars Crossers (defined here as perihelion <1.67 AU) with $H \geq 16$, signal-to-noise ratio at $1\mu\text{m} \geq 20$ and olivine to pyroxene ratio ≥ 0.65 (described in Sec 3.2) most of which are publicly available from the SMASS and MITHNEOS programs (Bus and Binzel 2002; Binzel et al. 2004b; DeMeo et al. 2009; Binzel et al. 2019a; Marsset et al. 2022) as well as other published literature (Wisniewski 1991; Hicks et al. 1998; Binzel et al. 2001a,b; Whiteley 2001; Bus and Binzel 2002; Binzel et al. 2004b; Lazzarin et al. 2004; Binzel et al. 2004a; Rivkin et al. 2004; Lazzarin et al. 2005; Michelsen et al. 2006; Roberts et al. 2007; Hicks and Lawrence 2009; Binzel et al. 2009; de León et al. 2010; Hicks et al. 2010a; Hicks and Buratti 2010; Hicks et al. 2010b, 2011; Hasselmann et al. 2011; Hicks et al. 2012; Sanchez et al. 2013; Ieva et al. 2014; Kuroda et al. 2014; Thomas et al. 2014; Perna et al. 2016; Carry et al. 2016; Binzel et al. 2019a; Marsset et al. 2022). The full list of asteroids with their observation dates and visible and near-infrared data references are provided in the Supplementary Data. Most visible-wavelength observations were made between August 1993 and March 1999 using the 2.4-m (f/7.5) Hiltner or 1.3-m (f/7.6) McGraw–Hill reflecting telescopes at the MDM Observatory. Most near-infrared data were obtained using SpeX on the NASA IRTF (Rayner et al. 2003). Data collected through October 2021 were included in the analysis. New observations taken between October 2020 and October 2021 (SpeX runs sp273 through sp286) are newly published in this work. Observation and reduction details for SpeX data can be found in Marsset et al. (2022). A number of asteroids had near-infrared spectral measurements from multiple nights, in which case we keep the spectrum with the highest signal-to-noise ratio. The sample includes only objects with $H > 16$ which corresponds roughly to bodies <2 km across. We restrict the sample because most Q-types are found below that size. Spectral plots of the 477 asteroid spectra are provided in the Supplementary Data.

3. Methods

3.1. Taxonomic Classification of Spectra

Most data were given taxonomic assignments in previous work (Bus and Binzel 2002; Binzel et al. 2004b; DeMeo et al. 2009; Binzel et al. 2019a; Marsset et al. 2022), and we use the existing classifications for the spectra used in this work. New data were classified using the Bus-DeMeo classification system (DeMeo et al. 2009) (a classification tool is publicly available, smass.mit.edu/busdemeoclass.html) and visual inspection of spectral features as described in detail in Marsset et al. (2022). We include all S-complex objects in this work except for Sa-types which have much higher olivine contents and are not compositionally equivalent to ordinary chondrites (Cruikshank and Hartmann 1984; Sunshine et al. 2007).

We then more carefully distinguish between Q-types and the rest of the S-complex. For asteroids for which we have data over the full 0.5–2.45 μm range, we use the unambiguous classification result from the Bus-DeMeo system. For asteroids with near-infrared-only data in the 0.8–2.5 μm range for which the classification system does not provide a unique result, we use the method from DeMeo et al. (2014) to determine the appropriate designation within the S-complex or Q-type.

For the analysis in this work we focus on the ratio of fresh-to-weathered asteroids, which is represented taxonomically as the ratio of Q-types to S-types (Q/S ratio). As is done in DeMeo et al. (2014), a weighting of 0.5 is given to objects assigned as “Q:” (degenerate between Sq and Q). Any object classified as S, Sq, or Sr is grouped as “S”. Any object classified as Q is kept as Q.

3.2. Mineralogic Modeling: Shkuratov Method

We performed a mineralogical analysis of S-complex spectra using the Shkuratov et al. (1999) radiative transfer model. The asteroid spectra were reddened using the empirical function from Brunetto et al. (2006), using their space weathering factor “Cs” as a free parameter in the fitting process. Our spectra were modeled following the procedure described by Vernazza et al. (2008) and Binzel et al. (2019a). The output product of our Shkuratov modeling is an estimate for the ol/(ol+px) ratio that provides the best fit to the spectrum out to 1.9 μm . Model results are provided in Supplementary Material.

Because Q-types have spectra that are olivine-rich, similar to L- and LL-chondrites, we remove any S-complex spectra with low olivine to pyroxene ratios (ol/(ol+opx) < 0.65) from the analysis. The resulting dataset includes 477 asteroids.

3.3. Minimum Orbit Intersection Distance Calculation

We calculate the orbit and Minimum Orbit Intersection Distance (MOID) to Venus, Earth, and Mars over the past 500,000 years. This is done in the same manner as Binzel et al. (2010) and DeMeo et al. (2014) using the `swift_rmvs3` code from Levison and Duncan (1994) with a 3.65-day time step and output values computed at 50-year intervals, accounting for the eight planets Mercury to Neptune. Our integrations for each asteroid included six additional clones, test particles with the same initial position, offset with velocities differing by $\pm 6 \times 10^{-6}$ astronomical unit (AU) per year in each Cartesian component. These clones are important to evaluate the range of potential orbital evolutions. From these orbital histories we find the MOID for Venus, Earth, and Mars.

We then define a number of “MOID classes” based on the planets for which an asteroid has a close approach. We define a “close approach” as a MOID smaller than 10 planetary radii of the given planet. The MOID classes include: V+E+M (encounters with Venus, Earth, and Mars), V+E (Venus and Earth), Earth, E+M (Earth and Mars), Mars, and None (No encounters with planets). Asteroids in the “None” class are unlikely to have encountered a planet over the 500,000 year integration. Among a sample of 225 NEOs that were unlikely to have encountered a planet (“None” MOID class) over the past 500,000 years, we ran a longer integration test of 2,000,000 years and found 218 (97%) remained in that class.

Half of the sample crossed all planets (V+E+M), the Earth + Mars and Mars-only populations each accounted for ~20%, and the Venus + Earth and None populations each made up 6% and 3% as shown in Fig. 1. There were very few asteroids in our sample that only crossed Earth, and none that only crossed Venus.

4. Results

Using the dataset of 477 S-complex asteroids with ol/(ol+opx) ratios > 0.65 we explore orbital and physical trends with the Q/S ratio (defined in Sec. 3.1) to interpret possible refreshing mechanisms. In Fig. 2 we plot the running Q/S

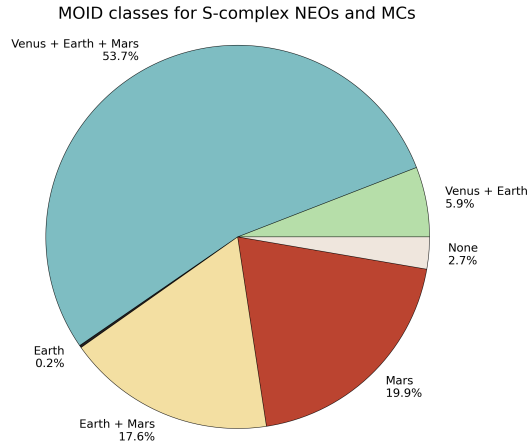


Figure 1: The number of NEOs and MCs that fall into each MOID class. For example, 54% of our sample (256 objects) encounter the orbits of Venus, Earth and Mars (V+E+M class), whereas 3% of our sample (13 objects) do not encounter any of the planets (None class).

ratio as a function of perihelion, H magnitude, and inclination. Below, we describe the Q/S trend for each of them.

Q/S Trend by size: As shown in Fig. 2 the Q/S trend with H magnitude is relatively flat over the H magnitude range of 16–18. There is an increase in the Q/S ratio near H magnitude of 19, and for $H \geq 19.5$ the Q/S ratio decreases linearly. The Q/S ratio near the minima and maximum on this plot is 0.29 ± 0.03 ($H=17.0-18.0$, 86 objects), 0.45 ± 0.05 ($H=18.7-19.7$, 80 objects), and 0.17 ± 0.02 ($H \geq 21.0$, 83 objects). There is a $>1\sigma$ difference between the $H=17.0-18.0$ region and both other regions. There is a $>3\sigma$ difference between the maximum at $H \sim 19$ and $H > 21.0$ (this 3σ difference is not visually apparent in Fig. 2 with the large box size of 125).

Binzel et al. (2004b) and Thomas et al. (2012) show decreasing average S-complex slope with size, inferring a higher fraction of Q-types at smaller sizes. Using data from the Sloan Digital Sky Survey (SDSS, Ivezić et al. 2001), Thomas et al. (2012) analyze Main Belt Objects in the Koronis family up to $H \sim 15.3$, so there is no overlap with our data that start at $H > 16$. Graves et al. (2018) found a similar trend in the Flora family. The observations from Binzel et al. (2004b) span from 10 km to 0.4 meters, but the slope decrease happens mostly for diameters greater than 1 km ($H=16-17$) and levels off at smaller sizes. Our result is consistent with these works, showing that overall, there is an increase of fresher asteroids at smaller sizes down to H magnitude roughly 16, but we find a sharper increase in the Q/S ratio near $H \sim 19$ and a decreasing ratio at smaller sizes.

Q/S Trend by inclination: We find the Q/S ratio peaks between 3° and 6° , seen as the strong peak in the running Q/S ratio, centered at $i \sim 5^\circ$ in Fig. 2. The Q/S ratio drops off steeply at both higher and lower inclinations. The Q/S ratio is 0.17 ± 0.02 between $i=0-3^\circ$ (59 objects), 0.45 ± 0.04 between $i=3-6^\circ$ (99 objects), and 0.25 ± 0.02 between $i=6-10^\circ$ (122 objects). There is a 4σ difference between the $i=0-3^\circ$ and $i=3-6^\circ$ groups and a 3σ difference between the $i=3-6^\circ$ and $i=6-10^\circ$ groups.

Q/S Trend by perihelion: We see a clear trend of an increasing Q/S ratio with decreasing perihelion, as seen by many previous authors (e.g., Marchi et al. 2006; Devogèle et al. 2019; Binzel et al. 2019b). We find no Q-types with perihelia > 1.3 AU although our sample is relatively small at that distance (34 objects).

Q/S Trend by phase angle: We also see a clear trend of increasing Q/S with increasing phase angle, as was seen by DeMeo et al. (2014). This trend initially seems counter-intuitive because increasing phase angle should increase the spectral slope making an object less likely to be classified as Q-type. We find no correlation with phase angle and asteroid size. We find that phase angle and perihelion are correlated, as phase angle increases, perihelion decreases. Because the number of Q-types increases with decreasing perihelion, it is natural that as a by-product the average phase angle at which those bodies are observed increases.

Q/S Trend by MOID class: In Fig. 3 we plot the Q/S ratio by perihelion for each MOID class (defined by the

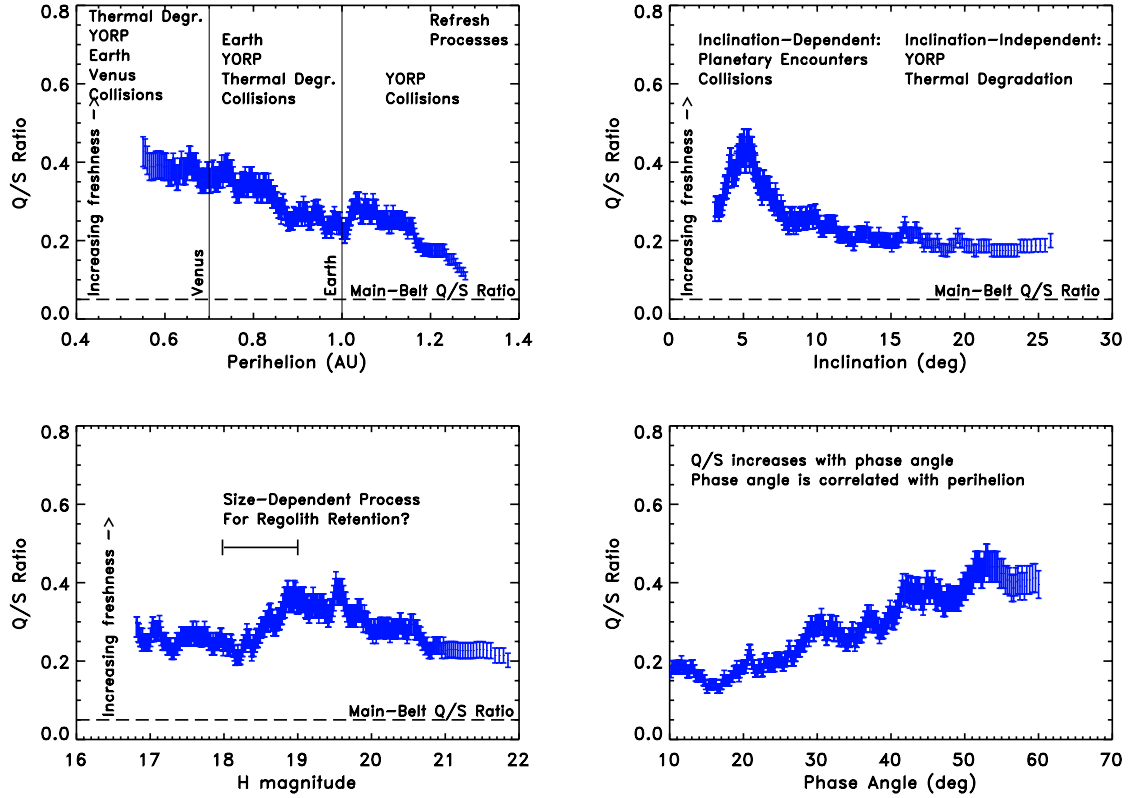


Figure 2: The running Q/S ratio for perihelion, H magnitude, inclination and phase angle for the 477 asteroids with $ol/(ol+opx) \geq 0.65$ with a box size of 125. Poisson errors are plotted as the Q/S ratio (y value) divided by the square root of n , where n is number of objects in the bin. The estimated main-belt Q/S ratio is from Lin et al. (2015) and represents a similar size range as this dataset. The observational phase angle and perihelion are correlated, with phase angle increasing as perihelion decreases.

planets the object could encounter, see Sec. 3.3). We see a trend where encounters with planets (including more and larger planets) has a higher Q/S ratio, but the overall perihelion trend appears to dominate these results. We note a few interesting trends:

- First, the Earth+Mars population has the opposite trend from the other classes and from the overall trend – there is a peak in the Q/S ratio near 1.1 AU and a minimum near 0.9 AU. There are 114 objects in this group. However, The average Q/S ratio of this population follows the overall perihelion trend.
- Second, the average Q/S ratio for the Mars class is 0.136 ± 0.014 and for the None class is 0.083 ± 0.023 . The ratios of the two classes differ by more than 1σ (using Poisson uncertainties) but less than 2σ . This result emphasizes that the role of Mars in surface refreshing is either small or zero (Carry et al. 2016; Devog le et al. 2019).
- Third, because the “None” population does have some Q-types, it represents a definitive baseline for Q-types created by processes other than planetary encounters.
- Fourth, the V+E (Venus- and Earth-crossing) average Q/S ratio is lower than V+E+M (Venus-, Earth- and Mars-crossing) ratio at the lowest perihelion distances, however, the two overall class averages are very similar.

Trends by source region: To look for trends as a function of source region, we use probabilities for an asteroid to enter the NEO region through a certain escape region—defined as a combination of mean-motion and/or secular resonances or as a group separated from other asteroids in orbital-element space—from the main asteroid belt as

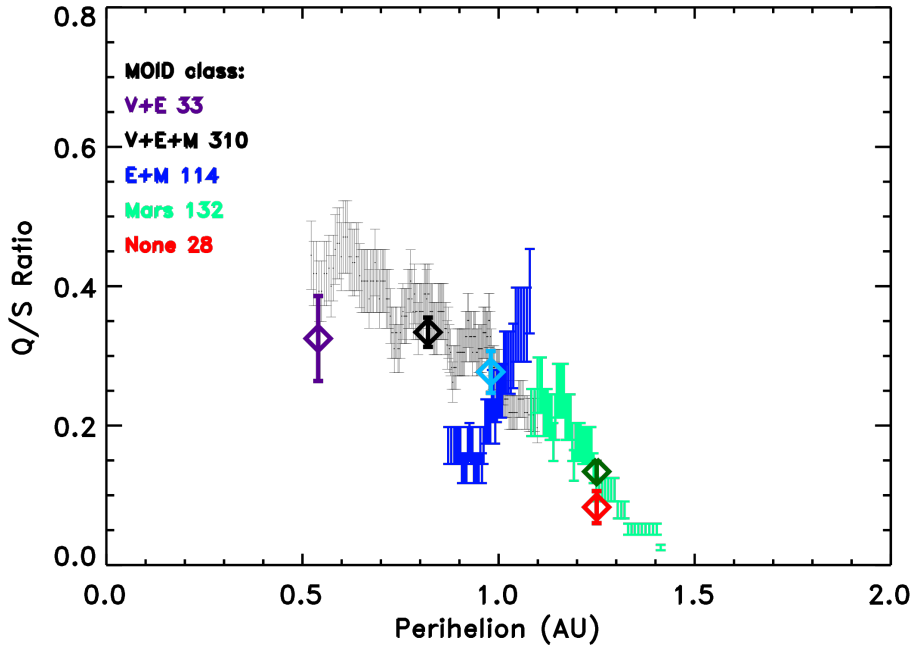


Figure 3: The running Q/S ratio with perihelion displayed by MOID class. Each class is plotted in a unique color as shown on the plot legend, and the number of objects in each class is also listed. Black includes objects that cross Venus, Earth, and Mars. Blue includes objects that cross Earth and Mars, and in green are objects that only cross Mars. The running mean box size is 81 for the V+E+M population and 41 for the others. We plot as a diamond the overall average Q/S ratio and perihelion for each MOID class including two additional groups that did not have enough data for a running ratio: the Venus + Earth population in purple and the None (crossing no planet) population in red.

predicted by the model of Granvik et al. (2018). We note that, for the resonance complexes, the probabilities do not necessarily correspond to the true source regions, but to the last location of a given asteroid just before it enters the NEO region. Marsset et al. (2022) calculated and published probabilities for most of the asteroids considered here and we have calculated the probabilities for the remaining ones using the same approach. Of the asteroids in our sample with high olivine content ($ol/(ol+opx) \geq 0.65$), 359 had $>50\%$ probability of entering the NEO region through the ν_6 resonance complex, representing 75% of our sample. 302 objects or 63% had $>70\%$ ν_6 probability. Of all the other escape regions considered by the model (the Hungaria, Phocaea, and JFC groups, and the 3:1, 5:2, and 2:1 resonance complexes) there were a negligible number of asteroids with $>70\%$ probability of coming from that escape region (less than 10 objects for each region). Hence we assign each of these NEOs that have a high olivine content the probability of originating from the ν_6 resonance complex.

In Fig. 4 we plot the Q/S ratio as a function of increasing ν_6 probability and find as the ν_6 probability increases, the Q/S ratio increases. However, there is a strong spike in the Q/S ratio for ν_6 probabilities $>80\%$. We also calculate an average age for each NEO by multiplying each source probability by the mean NEO lifetime from that source from Granvik et al. (2018). We find a peak in the Q/S ratio near 8 My corresponds with the higher probability of originating from the ν_6 (mean lifetime between 7.2 and 9.4 My).

5. Discussion

5.1. Discussion of Primary Q/S Trends

There are 4 primary trends with the Q/S ratio. Each refreshing mechanism (described in the Introduction, Sec. 1) is dependent on different factors, such as size, distance from the Sun, and close encounters with planets, and the dominant refreshing mechanisms should be able to explain one or more of these trends. We summarize the observed trends and dependencies in Table 1 and discuss these trends in the context of potential refreshing mechanisms.

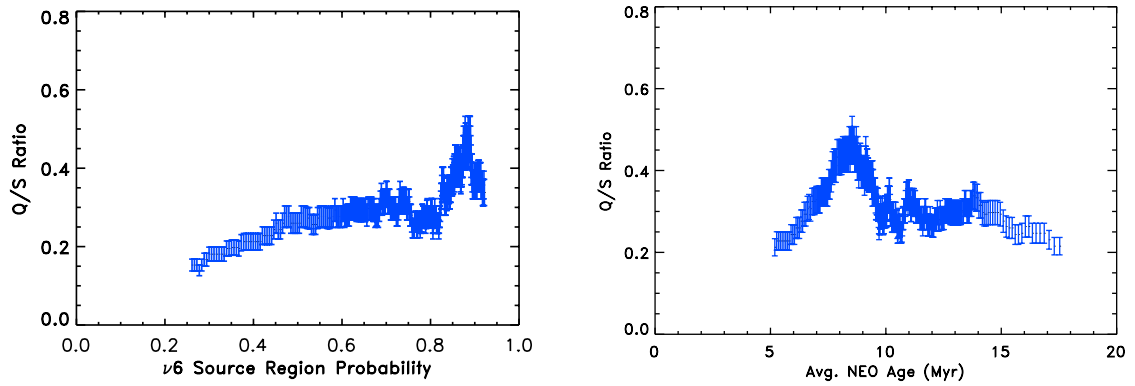


Figure 4: Left: The running Q/S ratio over the probability of being sourced from the ν_6 secular resonance. There is a spike in the Q/S ratio (more fresh bodies) for ν_6 source probabilities $>80\%$. Right: The Q/S ratio as a function of average NEO age calculated as the sum of a body's probability from each source region time the mean NEO lifetime from that region from Granvik et al. (2018). The mean life time from the ν_6 is 9.4 and 7.2 My for perihelia less than and greater than 1.3 AU, respectively. The peak in Q/S ratio near 8 My corresponds with the higher probability of originating from the ν_6 .

Table 1
Q/S Trends with Orbital and Physical Properties

Property	Observed Q/S Trend	Dependent Mechanism	Independent Mechanism	References
Size	Dependent: Q/S increases for decreasing size for $H < 16$, peaks near $H \sim 19$ and decreases at smaller sizes	YORP	Encounters, Collisions, Thermal Degradation	Binzel et al. (2004b); Mothé-Diniz and Nesvorný (2008); Rivkin et al. (2011); Thomas et al. (2011, 2012); Lin et al. (2015); Carry et al. (2016); Graves et al. (2018), This Work.
Inclination	Dependent: Q/S peaks at $3-6^\circ$	Encounter, Collisions	YORP, Thermal Degradation	Dell'Oro et al. (2011), This Work.
Perihelion	Dependent: Q/S increases for $q \lesssim 0.9$ AU. Independent for $q \gtrsim 0.9$ AU.	Thermal Degradation, Encounter, Collisions	YORP	Marchi et al. (2006); Devogèle et al. (2019); Binzel et al. (2019b), This Work.
MOID	Dependent? MOID effects not easily distinguished from perihelion effects	Encounter	YORP, Collisions, Thermal Degradation	Nesvorný et al. (2010); Binzel et al. (2010); DeMeo et al. (2014); Carry et al. (2016); Devogèle et al. (2019), This Work.

First, the Q/S ratio increases at smaller sizes down to $H \lesssim 16$, peaks at $H \sim 19$ and then decreases with increasing H . The lowest Q/S ratio is seen at the smallest sizes, $H \geq 21.0$. YORP is size-dependent and is more effective at smaller sizes, particularly in the kilometer size range and smaller (Bottke et al. 2006). Collisions are dependent on size to some extent as well. While the rate of collisions is roughly size-independent (in fact it increases with cross-sectional area or size), the larger the body the less effective a micro-impact will be at global surface refreshing. Planetary encounters and thermal degradation should not be size dependent. Graves et al. (2018) modeled the spectral slope versus size (H magnitude) trend for asteroids for planetary encounters and YORP (modeling refreshing happening at the fission spin rate, though it could happen more often). They found YORP could adequately model the spectral slope trend with H -magnitude trend, but planetary encounters could not.

We find a peak in the Q/S ratio near $H \sim 19$ (see Fig. 2). One possible explanation is that we are seeing the transition between “large” NEOs which are all rubble piles and smaller bodies some of which are monoliths that can surpass the

spin-barrier limit (Pravec and Harris 2000; Warner et al. 2009). As the number of regolith-free monoliths increases (at smaller sizes), the Q/S ratio would decrease. Additionally, with decreasing size, decreasing gravity decreases regolith retention. There are two competing forces between monolith creation from fission from YORP spinup, and regolith creation from thermal degradation.

Second, the Q/S ratio increases with decreasing perihelion distance. Thermal degradation should scale as a power law with distance from the Sun, meaning more fresh surfaces at lower perihelia. Graves et al. (2019) modeled thermal degradation as a method of reducing spectral slope (refreshing a surface) and was able to adequately reproduce the observed trend. The YORP effect should be distance independent because both YORP and space weathering are dependent on solar radiation and should thus scale at the same rate with distance (Graves et al. 2018). Collisions are most effective for bodies on orbits that spend more time in the Main Belt, and so would not cause the observed perihelion trend. Planetary encounters are indirectly related to perihelion, but require a unique MOID signature with the planets to identify it. At lower perihelia more (perhaps all) processes are at work, and thus the combined forces would also naturally increase the abundance of fresh surfaces. Each process may have a different physical refreshing effect. Thermal fatigue takes over to break down boulders, creating new, fresh regolith at a very fast rate. YORP could be massively shedding outer layers, exposing fresh surface. Planetary encounters may be overturning existing, weathered grains, exposing fresh material.

Third, our analysis reveals that the Q/S ratio is significantly higher at inclinations between 3 and 6° than at lower and higher inclinations. We are able to dismiss the processes of YORP and thermal degradation, as these have no dependence on inclination. We have three possible interpretations of this trend:

- Planetary encounters are very strongly coupled to inclination, where the dynamical likelihood of planetary encounters scales with $1/\sin(i)$ (Wetherill 1967). For asteroids evolved out of the main belt into planet crossing orbits, planetary encounters dominate over asteroid-asteroid collisions (Nesvorný et al. 2010). Planetary encounters, however, are most efficient for bodies on orbits with inclinations near zero. If the signal we see at low inclinations ($i \sim 5^\circ$) is due to planetary encounters then, the drop for $i \lesssim 5^\circ$ indicates depletion of the population either by collision or frequent encounters that fling the bodies into a new orbit (higher i). At $i=0^\circ$ planet crossing collision is effectively inevitable. The sample cannot peak near 0° as the survival time near 0 is too short.
- The inclination signal is an indicator of NEO average lifetime. The median inclination of the inner belt is around 5.2° (as calculated from MPCORB.dat from the Minor Planet Center in May 2022). The Flora family is also centered near $3\text{--}6^\circ$ (Nesvorný et al. 2015). Flora is a major source of NEOs through the ν_6 resonance, we also see a spike in the Q/S ratio for objects with very high probability ($>85\%$) of coming through the ν_6 (Fig. 4). NEOs from the ν_6 have a much longer mean lifetime (7-9 My) than NEOs originating from the J3:1 (2 My) or J5:2 (0.05 My) (average NEO lifetimes from Granvik et al. 2018). The longer lifetime indicates more time for resurfacing processes (any or all of them) to take place.
- Collisions: Dell'Oro et al. (2011) found a correlation between NEO slopes and the estimated intensity of collisional processes. While those authors do not note a direct correlation between slope and inclination, they show collisions are more frequent for low inclinations and for aphelia of about 2.75 AU. In a survey of 150 small MBAs, Lin et al. (2015) find the Q/S ratio to be less than 5% down to an observational limit of 1km. The relative paucity of Q-types among small MBAs indicates that while asteroid-asteroid encounters create some resurfacing, this process operates at a very low background level. The Flora family, specifically, is a source of S-type NEOs (Nesvorný et al. 2002), but is not a major source of small meteorite-sized bodies (Vernazza et al. 2008) – only 80% of meteorite falls are ordinary chondrite, but only 10% of falls are LL-type (Flora-like compositions). Both the low fraction of Q-types among the Flora family and the paucity of small meteorite-sized bodies (meter size or smaller to cause refreshing but not total disruption) from Flora argues against there being a significant population of small bodies in that family causing refreshing collisions among NEOs.

Fourth, the Q/S ratio is higher for objects that have the possibility of encounter with Earth and Venus versus Mars or no planet. This trend is more challenging to interpret uniquely because it strongly overlaps with the perihelion trend. Objects that interact with Venus and Earth naturally have lower perihelia on average than those that do not. Previous work that found Q-types had higher probabilities of interacting with planets than S-types (Binzel et al. 2010; Carry et al. 2016) were biased because they included higher perihelia S-types (Graves et al. 2019). Additionally, Graves et al. (2018) and Graves et al. (2019) could not satisfactorily model the observed H magnitude and perihelion

trends by planetary encounters. The sharp decrease in fresh surfaces for objects in the Earth + Mars MOID class in Fig. 3 is curious, but may be a signal of the dynamical influx from the ν_6 resonance, where first-time encounters are particularly efficient at exposing fresh material. Bodies in this region are in a very active phase of Earth encounters, where fresh material is frequently exposed, then sautéed, until the upper regolith layer is saturated by space weathering. Alternatively or in addition, repeated encounters could lead to a loss of regolith during an interval where an object is strongly coupled to the planet's orbit.

There is observational evidence that YORP (correlated to H magnitude) and thermal degradation (correlated to perihelion) and collisions (correlated to inclination) each play a role in surface refreshing. The existence of fresh surfaces in the main belt further supports the role of YORP and collisions. Planetary encounters likely plays a role, however, the existing orbital trends can be explained by other refreshing mechanisms, and we are unable to uniquely distinguish encounters as a mechanism in this work. We see support for the role of planetary encounters in the peak in the Q/S ratio at low inclinations near 5° (Fig. 2).

5.2. Discussion of Caveats and Other Explanations

Compositional Homogeneity Caveat: Space weathering effects vary based on the composition of the body. In this work, we have attempted to use a relatively compositionally homogenous sample that includes S-complex bodies with high olivine content ($\text{ol}/(\text{ol}+\text{opx}) \geq 0.65$). Additionally, a large portion of this sample is likely sourced from the ν_6 resonance which is also dominated by the large Flora family. However, it is still possible, that there are biases in our trends based on different populations of NEOs being sourced from different regions of the of the Main Belt.

Grain Size Alternative Explanation: How significant is the effect of grain size on an asteroid surface? Hasegawa et al. (2019) performed irradiation experiments of ordinary chondrite meteorites of varying grain sizes and found that the spectral slopes remained low for large-grained irradiated samples. They suggest that a significant fraction of Q-types could simply be weathered surfaces with large grains.

Some smaller asteroids are monoliths and may not have a significant regolith layer (Pravec and Harris 2000). Perhaps some smaller bodies have surfaces dominated by 30-cm boulders, the size limit at which thermal degradation is not longer effective. Spectra of larger grains and slabs typically have weaker band depths compared to smaller grains (e.g., Cloutis et al. 2011; Krämer Ruggiu et al. 2021; DeMeo et al. 2022), yet Q-type asteroids have both low spectral slopes and deep $1\mu\text{m}$ absorption bands. An investigation of other band parameters other than slope such as width and depth would should help constrain the role grain size plays in our interpretation of Q-type asteroids and their relative fraction among the S-complex.

6. Conclusion

We find 4 trends with the Q/S ratio representing fresh versus weathered surfaces with size, perihelion, inclination, and MOID. The complexity of these trends highlights that no single resurfacing mechanism can explain all of these trends, so multiple mechanisms are required.

These observational trends are:

- Size: The Q/S ratio increases at smaller sizes down to $H \lesssim 16$, then peaks near $H \sim 19$ after which the ratio decreases, revealing that there are fewer fresh surfaces at the smallest sizes, particularly smaller than $H > 21$.
- Perihelion: The Q/S ratio increases with decreasing perihelion. Our results and previous work have shown that the Q/S ratio is small, but non-zero for perihelia > 1.2 AU, including among Mars Crossers and the Main Asteroid Belt.
- Inclination: The Q/S ratio exhibits a strong peak for inclinations between $3-6^\circ$.
- MOID: The Q/S ratio is higher for objects that have the possibility of encounter with Earth and Venus versus Mars or no planet (low MOID). The major trends seen for MOID, however, can be easily confounded with the trend for perihelion.

The possible explanations for the observed trends (see Table 1):

- YORP may dominate the observed trend with size (Graves et al. 2018), but not with perihelion or inclination.
- Thermal degradation likely dominates the observed trend with perihelion (Graves et al. 2019).

- Planetary encounters are likely the dominant mechanism to explain the observed trend with inclination. Encounters could also explain the perihelion trend and Q/S ratio for objects with low MOIDs, however, most low perihelion asteroids (of any taxonomic class including Q or S) also have low MOIDs making it difficult to separate the effect of MOID from perihelion.
- Collisions could be responsible for producing Q-types at low inclinations and also at large distances such as in the Main Belt. They could also be size dependent because smaller bodies would be more likely to be globally resurfaced by a micro-impact compared to a larger body, although this has not yet been modeled at the population level.
- Grain size could play a role, with larger grains causing lower spectral slopes regardless of weathering level. Additional investigation of band parameters such as width, depth, and area would provide further constraints.

7. Acknowledgements

We thank David Nesvorný for helpful discussions that are always insightful. We also thank Vishnu Reddy and an anonymous referee for helpful reviews. Observations reported here were obtained at the NASA Infrared Telescope Facility, which is operated by the University of Hawaii under contract 80HQTR19D0030 with the National Aeronautics and Space Administration. The MIT component of this work is supported by NASA grant 80NSSC18K1004 and 80NSSC18K0849. SH was supported by the Hypervelocity Impact Facility (former name: The Space Plasma Laboratory), ISAS, JAXA. Any opinions, findings, and conclusions or recommendations expressed in this article are those of the authors and do not necessarily reflect the views of the National Aeronautics and Space Administration.

References

- Abe, M., Takagi, Y., Kitazato, K., Abe, S., Hiroi, T., Vilas, F., Clark, B.E., Abell, P.A., Lederer, S.M., Jarvis, K.S., Nimura, T., Ueda, Y., Fujiwara, A., 2006. Near-Infrared Spectral Results of Asteroid Itokawa from the Hayabusa Spacecraft. *Science* 312, 1334–1338. doi:[10.1126/science.1125718](https://doi.org/10.1126/science.1125718).
- Binzel, R.P., DeMeo, F.E., Turtelboom, E.V., Bus, S.J., Tokunaga, A., Burbine, T.H., Lantz, C., Polishook, D., Carry, B., Morbidelli, A., Birlan, M., Vernazza, P., Burt, B.J., Moskovitz, N., Slivan, S.M., Thomas, C.A., Rivkin, A.S., Hicks, M.D., Dunn, T., Reddy, V., Sanchez, J.A., Granvik, M., Kohout, T., 2019a. Compositional distributions and evolutionary processes for the near-Earth object population: Results from the MIT-Hawaii Near-Earth Object Spectroscopic Survey (MITHNEOS). *Icarus* 324, 41–76. doi:[10.1016/j.icarus.2018.12.035](https://doi.org/10.1016/j.icarus.2018.12.035), [arXiv:2004.05090](https://arxiv.org/abs/2004.05090).
- Binzel, R.P., DeMeo, F.E., Turtelboom, E.V., Bus, S.J., Tokunaga, A., Burbine, T.H., Lantz, C., Polishook, D., Carry, B., Morbidelli, A., Birlan, M., Vernazza, P., Burt, B.J., Moskovitz, N., Slivan, S.M., Thomas, C.A., Rivkin, A.S., Hicks, M.D., Dunn, T., Reddy, V., Sanchez, J.A., Granvik, M., Kohout, T., 2019b. Compositional distributions and evolutionary processes for the near-Earth object population: Results from the MIT-Hawaii Near-Earth Object Spectroscopic Survey (MITHNEOS). *Icarus* 324, 41–76. doi:[10.1016/j.icarus.2018.12.035](https://doi.org/10.1016/j.icarus.2018.12.035), [arXiv:2004.05090](https://arxiv.org/abs/2004.05090).
- Binzel, R.P., Harris, A.W., Bus, S.J., Burbine, T.H., 2001a. Spectral Properties of Near-Earth Objects: Palomar and IRTF Results for 48 Objects Including Spacecraft Targets (9969) Braille and (10302) 1989 ML. *Icarus* 151, 139–149. doi:[10.1006/icar.2001.6613](https://doi.org/10.1006/icar.2001.6613).
- Binzel, R.P., Morbidelli, A., Merothane, S., DeMeo, F.E., Birlan, M., Vernazza, P., Thomas, C.A., Rivkin, A.S., Bus, S.J., Tokunaga, A.T., 2010. Earth encounters as the origin of fresh surfaces on near-Earth asteroids. *Nature* 463, 331–334. doi:[10.1038/nature08709](https://doi.org/10.1038/nature08709).
- Binzel, R.P., Perozzi, E., Rivkin, A.S., Rossi, A., Harris, A.W., Bus, S.J., Valsecchi, G.B., Slivan, S.M., 2004a. Dynamical and compositional assessment of near-Earth object mission targets. *Meteoritics and Planetary Science* 39, 351–366. doi:[10.1111/j.1945-5100.2004.tb00098.x](https://doi.org/10.1111/j.1945-5100.2004.tb00098.x).
- Binzel, R.P., Rivkin, A.S., Bus, S.J., Sunshine, J.M., Burbine, T.H., 2001b. MUSES-C target asteroid (25143) 1998 SF36: A reddened ordinary chondrite. *Meteoritics and Planetary Science* 36, 1167–1172. doi:[10.1111/j.1945-5100.2001.tb01950.x](https://doi.org/10.1111/j.1945-5100.2001.tb01950.x).
- Binzel, R.P., Rivkin, A.S., Stuart, J.S., Harris, A.W., Bus, S.J., Burbine, T.H., 2004b. Observed spectral properties of near-Earth objects: results for population distribution, source regions, and space weathering processes. *Icarus* 170, 259–294. doi:[10.1016/j.icarus.2004.04.004](https://doi.org/10.1016/j.icarus.2004.04.004).
- Binzel, R.P., Rivkin, A.S., Thomas, C.A., Vernazza, P., Burbine, T.H., DeMeo, F.E., Bus, S.J., Tokunaga, A.T., Birlan, M., 2009. Spectral properties and composition of potentially hazardous Asteroid (99942) Apophis. *Icarus* 200, 480–485. doi:[10.1016/j.icarus.2008.11.028](https://doi.org/10.1016/j.icarus.2008.11.028).
- Bonanno, C., 2000. An analytical approximation for the MOID and its consequences. *Astronomy and Astrophysics* 360, 411–416.
- Botke, Jr., W.F., Vokrouhlický, D., Rubincam, D.P., Nesvorný, D., 2006. The Yarkovsky and Yorp Effects: Implications for Asteroid Dynamics. *Annual Review of Earth and Planetary Sciences* 34, 157–191. doi:[10.1146/annurev.earth.34.031405.125154](https://doi.org/10.1146/annurev.earth.34.031405.125154).
- Brunetto, R., Vernazza, P., Marchi, S., Birlan, M., Fulchignoni, M., Orosfin, V., Strazzulla, G., 2006. Modeling asteroid surfaces from observations and irradiation experiments: The case of 832 Karin. *Icarus* 184, 327–337. doi:[10.1016/j.icarus.2006.05.019](https://doi.org/10.1016/j.icarus.2006.05.019).
- Bus, S.J., Binzel, R.P., 2002. Phase II of the Small Main-Belt Asteroid Spectroscopic Survey, The Observations. *Icarus* 158, 106–145. doi:[10.1006/icar.2002.6857](https://doi.org/10.1006/icar.2002.6857).
- Carry, B., Solano, E., Eggl, S., DeMeo, F.E., 2016. Spectral properties of near-Earth and Mars-crossing asteroids using Sloan photometry. *Icarus* 268, 340–354. doi:[10.1016/j.icarus.2015.12.047](https://doi.org/10.1016/j.icarus.2015.12.047), [arXiv:1601.02087](https://arxiv.org/abs/1601.02087).
- Cloutis, E.A., Hiroi, T., Gaffey, M.J., Alexander, C.M.O.D., Mann, P., 2011. Spectral reflectance properties of carbonaceous chondrites: 1. CI chondrites. *Icarus* 212, 180–209. doi:[10.1016/j.icarus.2010.12.009](https://doi.org/10.1016/j.icarus.2010.12.009).

- Cruikshank, D.P., Hartmann, W.K., 1984. The Meteorite-Asteroid Connection: Two Olivine-Rich Asteroids. *Science* 223, 281–283. doi:[10.1126/science.223.4633.281](#).
- de León, J., Licandro, J., Serra-Ricart, M., Pinilla-Alonso, N., Campins, H., 2010. Observations, compositional, and physical characterization of near-Earth and Mars-crosser asteroids from a spectroscopic survey. *Astronomy and Astrophysics* 517, A23. doi:[10.1051/0004-6361/200913852](#).
- Delbo, M., Libourel, G., Wilkerson, J., Murdoch, N., Michel, P., Ramesh, K.T., Ganino, C., Verati, C., Marchi, S., 2014. Thermal fatigue as the origin of regolith on small asteroids. *Nature* 508, 233–236. doi:[10.1038/nature13153](#).
- Dell’Oro, A., Marchi, S., Paolicchi, P., 2011. Collisional evolution of near-Earth asteroids and refreshing of the space-weathering effects. *Monthly Notices of the Royal Astronomical Society* 416, L26–L30. doi:[10.1111/j.1745-3933.2011.01089.x](#).
- DeMeo, F.E., Binzel, R.P., Lockhart, M., 2014. Mars encounters cause fresh surfaces on some near-Earth asteroids. *Icarus* 227, 112–122. doi:[10.1016/j.icarus.2013.09.014](#), [arXiv:1309.4839](#).
- DeMeo, F.E., Binzel, R.P., Slivan, S.M., Bus, S.J., 2009. An extension of the Bus asteroid taxonomy into the near-infrared. *Icarus* 202, 160–180. doi:[10.1016/j.icarus.2009.02.005](#).
- DeMeo, F.E., Burt, B.J., Marsset, M., Polishook, D., Burbine, T.H., Carry, B., Binzel, R.P., Vernazza, P., Reddy, V., Tang, M., Thomas, C.A., Rivkin, A.S., Moskovitz, N.A., Slivan, S.M., Bus, S.J., 2022. Connecting asteroids and meteorites with visible and near-infrared spectroscopy. *Icarus* 380, 114971. doi:[10.1016/j.icarus.2022.114971](#), [arXiv:2202.13797](#).
- Devogèle, M., Moskovitz, N., Thirouin, A., Gustaffson, A., Magnuson, M., Thomas, C., Willman, M., Christensen, E., Person, M., Binzel, R., Polishook, D., DeMeo, F., Hinkle, M., Trilling, D., Mommert, M., Burt, B., Skiff, B., 2019. Visible Spectroscopy from the Mission Accessible Near-Earth Object Survey (MANOS): Taxonomic Dependence on Asteroid Size. *Astronomical Journal* 158, 196. doi:[10.3847/1538-3881/ab43dd](#), [arXiv:1909.04788](#).
- Granvik, M., Morbidelli, A., Jedicke, R., Bolin, B., Bottke, W.F., Beshore, E., Vokrouhlický, D., Delbò, M., Michel, P., 2016. Super-catastrophic disruption of asteroids at small perihelion distances. *Nature* 530, 303–306. doi:[10.1038/nature16934](#).
- Granvik, M., Morbidelli, A., Jedicke, R., Bolin, B., Bottke, W.F., Beshore, E., Vokrouhlický, D., Nesvorný, D., Michel, P., 2018. Debaised orbit and absolute-magnitude distributions for near-Earth objects. *Icarus* 312, 181–207. doi:[10.1016/j.icarus.2018.04.018](#), [arXiv:1804.10265](#).
- Graves, K.J., Minton, D.A., Hirabayashi, M., DeMeo, F.E., Carry, B., 2018. Resurfacing asteroids from YORP spin-up and failure. *Icarus* 304, 162–171. doi:[10.1016/j.icarus.2017.08.025](#).
- Graves, K.J., Minton, D.A., Molaro, J.L., Hirabayashi, M., 2019. Resurfacing asteroids from thermally induced surface degradation. *Icarus* 322, 1–12. doi:[10.1016/j.icarus.2019.01.003](#).
- Hapke, B., 1965. Effects of a Simulated Solar Wind on the Photometric Properties of Rocks and Powders. *Annals of the New York Academy of Sciences* 123, 711–721. doi:[10.1111/j.1749-6632.1965.tb20395.x](#).
- Hapke, B., 1981. Bidirectional reflectance spectroscopy. I. Theory. *Journal of Geophysical Research* 86, 4571–4586.
- Hapke, B., 2001. Space weathering from Mercury to the asteroid belt. *Journal of Geophysical Research* 106, 10039–10074. doi:[10.1029/2000JE001338](#).
- Hapke, B.W., Cohen, A.J., Cassidy, W.A., Wells, E.N., 1970. Solar Radiation Effects in Lunar Samples. *Science* 167, 745. doi:[10.1126/science.167.3918.745](#).
- Hasegawa, S., Hiroi, T., Ohtsuka, K., Ishiguro, M., Kuroda, D., Ito, T., Sasaki, S., 2019. Q-type asteroids: Possibility of non-fresh weathered surfaces. *PASJ* 71, 103. doi:[10.1093/pasj/psz088](#), [arXiv:1907.08266](#).
- Hasselmann, P.H., Carvano, J.M., Lazzaro, D., 2011. SDSS-based Asteroid Taxonomy V1.0. NASA Planetary Data System, EAR–A–I0035–5–SDSSTAX–V1.0.
- Hicks, M., Buratti, B., 2010. Palomar Spectroscopy of the Potentially Hazardous Asteroids 2010 MF1 and 138404 (2000 HA24). *The Astronomer’s Telegram* 2822, 1.
- Hicks, M., Gerhart, C., Strojia, C., Teague, S., 2011. Palomar Spectroscopy of Near-Earth Asteroids 2004 SV55, 2000 SP43, 3988 (1986 LA), 1036 Ganymed, and 2002 AG29. *The Astronomer’s Telegram* 3678, 1.
- Hicks, M., Lawrence, K., 2009. Planetary radar targets 1999 AP10, 2000 TO64, 2000 UJ1, and 2000 XK44: Four S-complex near-Earth asteroids. *The Astronomer’s Telegram* 2323, 1.
- Hicks, M., Lawrence, K., Benner, L., 2010a. Palomar Spectroscopy of 2001 FM129, 2004 FG11, and 2005 YU55. *The Astronomer’s Telegram* 2571, 1.
- Hicks, M., Teague, S., Strojia, C., Dombroski, D., Davtyan, T., 2012. Physical Characterization of the Potentially Hazardous Asteroid 2011 WV134. *The Astronomer’s Telegram* 4251, 1.
- Hicks, M., Truong, T., Somers, J., 2010b. Broad-band photometry of the near-Earth asteroid 154029 (2002 CY46): An unusually steep solar phase curve and evidence for complex rotation. *The Astronomer’s Telegram* 2859, 1.
- Hicks, M.D., Fink, U., Grundy, W.M., 1998. The Unusual Spectra of 15 Near-Earth Asteroids and Extinct Comet Candidates. *Icarus* 133, 69–78. doi:[10.1006/icar.1998.5911](#).
- Hirabayashi, M., 2015. Failure modes and conditions of a cohesive, spherical body due to YORP spin-up. *Monthly Notices of the Royal Astronomical Society* 454, 2249–2257. doi:[10.1093/mnras/stv2017](#), [arXiv:1508.06913](#).
- Hiroi, T., Abe, M., Kitazato, K., Abe, S., Clark, B.E., Sasaki, S., Ishiguro, M., Barnouin-Jha, O.S., 2006. Developing space weathering on the asteroid 25143 Itokawa. *Nature* 443, 56–58. doi:[10.1038/nature05073](#).
- Hiroi, T., Pieters, C.M., 1992. Effects of grain size and shape in modeling reflectance spectra of mineral mixtures. *Lunar and Planetary Science Conference Proceedings* 22, 313–325.
- Ieva, S., Dotto, E., Perna, D., Barucci, M.A., Bernardi, F., Fornasier, S., De Luise, F., Perozzi, E., Rossi, A., Brucato, J.R., 2014. Low delta-V near-Earth asteroids: A survey of suitable targets for space missions. *Astronomy and Astrophysics* 569, A59. doi:[10.1051/0004-6361/201322283](#), [arXiv:1406.5027](#).
- Ishiguro, M., Hiroi, T., Tholen, D.J., Sasaki, S., Ueda, Y., Nimura, T., Abe, M., Clark, B.E., Yamamoto, A., Yoshida, F., Nakamura, R., Hirata, N.,

- Miyamoto, H., Yokota, Y., Hashimoto, T., Kubota, T., Nakamura, A.M., Gaskell, R.W., Saito, J., 2007. Global mapping of the degree of space weathering on asteroid 25143 Itokawa by Hayabusa/AMICA observations. *Meteoritics and Planetary Science* 42, 1791–1800. doi:[10.1111/j.1945-5100.2007.tb00538.x](#).
- Ivezić, Ž., Tabachnik, S., Rafikov, R., Lupton, R.H., Quinn, T., Hammergren, M., Eyer, L., Chu, J., Armstrong, J.C., Fan, X., Finlator, K., Geballe, T.R., Gunn, J.E., Hennessy, G.S., Knapp, G.R., Leggett, S.K., Munn, J.A., Pier, J.R., Rockosi, C.M., Schneider, D.P., Strauss, M.A., Yanny, B., Brinkmann, J., Csabai, I., Hindsley, R.B., Kent, S., Lamb, D.Q., Margon, B., McKay, T.A., Smith, J.A., Waddell, P., York, D.G., SDSS Collaboration, 2001. Solar System Objects Observed in the Sloan Digital Sky Survey Commissioning Data. *Astronomical Journal* 122, 2749–2784. doi:[10.1086/323452](#), [arXiv:astro-ph/0105511](#).
- Johnson, T.V., Fanale, F.P., 1973. Optical Properties of Carbonaceous Chondrites and Their Relationship to Asteroids. *Journal of Geophysical Research* 78, 8507–8518. doi:[10.1029/JB078i035p08507](#).
- Krämer Ruggiu, L., Beck, P., Gattacceca, J., Eschrig, J., 2021. Visible-infrared spectroscopy of ungrouped and rare meteorites brings further constraints on meteorite-asteroid connections. *Icarus* 362, 114393. doi:[10.1016/j.icarus.2021.114393](#), [arXiv:2105.01900](#).
- Kuroda, D., Ishiguro, M., Takato, N., Hasegawa, S., Abe, M., Tsuda, Y., Sugita, S., Usui, F., Hattori, T., Iwata, I., Imanishi, M., Terada, H., Choi, Y.J., Watanabe, S.i., Yoshikawa, M., 2014. Visible-wavelength spectroscopy of subkilometer-sized near-Earth asteroids with a low delta-v. *PASJ* 66, 51. doi:[10.1093/pasj/psu041](#).
- Lazzarin, M., Marchi, S., Barucci, M.A., Di Martino, M., Barbieri, C., 2004. Visible and near-infrared spectroscopic investigation of near-Earth objects at ESO: first results. *Icarus* 169, 373–384. doi:[10.1016/j.icarus.2003.12.023](#).
- Lazzarin, M., Marchi, S., Magrin, S., Licandro, J., 2005. Spectroscopic investigation of near-Earth objects at Telescopio Nazionale Galileo. *Monthly Notices of the Royal Astronomical Society* 359, 1575–1582. doi:[10.1111/j.1365-2966.2005.09006.x](#).
- Levison, H.F., Duncan, M.J., 1994. The long-term dynamical behavior of short-period comets. *Icarus* 108, 18–36. doi:[10.1006/icar.1994.1039](#).
- Lin, H.W., Yoshida, F., Chen, Y.T., Ip, W.H., Chang, C.K., 2015. A search for subkilometer-sized ordinary chondrite like asteroids in the main-belt. *Icarus* 254, 202–212. doi:[10.1016/j.icarus.2015.04.007](#), [arXiv:1504.01543](#).
- Marchi, S., Magrin, S., Nesvorný, D., Paolicchi, P., Lazzarin, M., 2006. A spectral slope versus perihelion distance correlation for planet-crossing asteroids. *Monthly Notices of the Royal Astronomical Society* 368, L39–L42. doi:[10.1111/j.1745-3933.2006.00152.x](#).
- Marsset, M., DeMeo, F.E., Binzel, R.P., Bus, S.J., Burbine, T.H., Burt, B., Moskovitz, N., Polishook, D., Rivkin, A.S., Slivan, S.M., Thomas, C., 2020. Twenty Years of SpeX: Accuracy Limits of Spectral Slope Measurements in Asteroid Spectroscopy. *Astrophysical Journal* 247, 73. doi:[10.3847/1538-4365/ab7b5f](#), [arXiv:2004.05158](#).
- Marsset, M., DeMeo, F.E., Burt, B., Polishook, D., Binzel, R.P., Granvik, M., Vernazza, P., Carry, B., Bus, S.J., Slivan, S.M., Thomas, C.A., Moskovitz, N.A., Rivkin, A.S., 2022. The Debaised Compositional Distribution of MITHNEOS: Global Match between the Near-Earth and Main-belt Asteroid Populations, and Excess of D-type Near-Earth Objects. *Astronomical Journal* 163, 165. doi:[10.3847/1538-3881/ac532f](#), [arXiv:2202.13796](#).
- Michelsen, R., Nathues, A., Lagerkvist, C.I., 2006. Spectroscopy of near-Earth asteroids. *Astronomy and Astrophysics* 451, 331–337. doi:[10.1051/0004-6361:20040443](#).
- Molaro, J.L., Byrne, S., Le, J.L., 2017. Thermally induced stresses in boulders on airless body surfaces, and implications for rock breakdown. *Icarus* 294, 247–261. doi:[10.1016/j.icarus.2017.03.008](#), [arXiv:1703.03085](#).
- Moskovitz, N.A., 2012. Colors of dynamically associated asteroid pairs. *Icarus* 221, 63–71. doi:[10.1016/j.icarus.2012.07.011](#), [arXiv:1207.3799](#).
- Moskovitz, N.A., Fatka, P., Farnocchia, D., Devogèle, M., Polishook, D., Thomas, C.A., Mommert, M., Avner, L.D., Binzel, R.P., Burt, B., Christensen, E., DeMeo, F., Hinkle, M., Hora, J.L., Magnusson, M., Matson, R., Person, M., Skiff, B., Thirouin, A., Trilling, D., Wasserman, L.H., Willman, M., 2019. A common origin for dynamically associated near-Earth asteroid pairs. *Icarus* 333, 165–176. doi:[10.1016/j.icarus.2019.05.030](#), [arXiv:1905.12058](#).
- Mothé-Diniz, T., Jasnin, F.L., Carvano, J.M., Lazzaro, D., Nesvorný, D., Ramirez, A.C., 2010. Re-assessing the ordinary chondrites paradox. *Astronomy and Astrophysics* 514, A86. doi:[10.1051/0004-6361/200913842](#).
- Mothé-Diniz, T., Nesvorný, D., 2008. Visible spectroscopy of extremely young asteroid families. *Astronomy and Astrophysics* 486, L9–L12. doi:[10.1051/0004-6361:200809934](#).
- Nakamura, T., Noguchi, T., Tanaka, M., Zolensky, M.E., Kimura, M., Tsuchiyama, A., Nakato, A., Ogami, T., Ishida, H., Uesugi, M., Yada, T., Shirai, K., Fujimura, A., Okazaki, R., Sandford, S.A., Ishibashi, Y., Abe, M., Okada, T., Ueno, M., Mukai, T., Yoshikawa, M., Kawaguchi, J., 2011. Itokawa Dust Particles: A Direct Link Between S-Type Asteroids and Ordinary Chondrites. *Science* 333, 1113–1115. URL: [http://adsabs.harvard.edu/abs/2011Sci...333.1113N](#), doi:[10.1126/science.1207758](#).
- Nesvorný, D., Bottke, W.F., Vokrouhlický, D., Chapman, C.R., Rafkin, S., 2010. Do planetary encounters reset surfaces of near Earth asteroids? *Icarus* 209, 510–519. doi:[10.1016/j.icarus.2010.05.003](#), [arXiv:1005.3526](#).
- Nesvorný, D., Brož, M., Carruba, V., 2015. Identification and Dynamical Properties of Asteroid Families, in: *Asteroids IV*, pp. 297–321. doi:[10.2458/azu_uapress_9780816532131-ch016](#).
- Nesvorný, D., Jedicke, R., Whiteley, R.J., Ivezić, Ž., 2005. Evidence for asteroid space weathering from the Sloan Digital Sky Survey. *Icarus* 173, 132–152. doi:[10.1016/j.icarus.2004.07.026](#).
- Nesvorný, D., Morbidelli, A., Vokrouhlický, D., Bottke, W.F., Brož, M., 2002. The Flora Family: A Case of the Dynamically Dispersed Collisional Swarm? *Icarus* 157, 155–172. doi:[10.1006/icar.2002.6830](#).
- Perna, D., Dotto, E., Ieva, S., Barucci, M.A., Bernardi, F., Fornasier, S., De Luise, F., Perozzi, E., Rossi, A., Mazzotta Epifani, E., Micheli, M., Deshapriya, J.D.P., 2016. Grasping the Nature of Potentially Hazardous Asteroids. *Astronomical Journal* 151, 11. doi:[10.3847/0004-6256/151/1/11](#).
- Pieters, C.M., Ammannito, E., Blewett, D.T., Denevi, B.W., de Sanctis, M.C., Gaffey, M.J., Le Corre, L., Li, J.Y., Marchi, S., McCord, T.B., McFadden, L.A., Mittlefehldt, D.W., Nathues, A., Palmer, E., Reddy, V., Raymond, C.A., Russell, C.T., 2012. Distinctive space weathering on Vesta from regolith mixing processes. *Nature* 491, 79–82. doi:[10.1038/nature11534](#).

- Polishook, D., Moskovitz, N., Binzel, R.P., DeMeo, F.E., Vokrouhlický, D., Žižka, J., Oszkiewicz, D., 2014. Observations of “fresh” and weathered surfaces on asteroid pairs and their implications on the rotational-fission mechanism. *Icarus* 233, 9–26. doi:[10.1016/j.icarus.2014.01.014](https://doi.org/10.1016/j.icarus.2014.01.014), [arXiv:1401.4465](https://arxiv.org/abs/1401.4465).
- Pravec, P., Harris, A.W., 2000. Fast and Slow Rotation of Asteroids. *Icarus* 148, 12–20. doi:[10.1006/icar.2000.6482](https://doi.org/10.1006/icar.2000.6482).
- Rayner, J.T., Toomey, D.W., Onaka, P.M., Denault, A.J., Stahlberger, W.E., Vacca, W.E., Cushing, M.C., Wang, S., 2003. Spex: A medium-resolution 0.8–5.5 micron spectrograph and imager for the nasa infrared telescope facility. *Astron. Soc. of the Pacific* 115, 362–382.
- Reddy, V., Dunn, T.L., Thomas, C.A., Moskovitz, N.A., Burbine, T.H., 2015. Mineralogy and Surface Composition of Asteroids. pp. 43–63. doi:[10.2458/azu_uapress_9780816532131-ch003](https://doi.org/10.2458/azu_uapress_9780816532131-ch003).
- Richardson, J.E., Melosh, H.J., Greenberg, R.J., O’Brien, D.P., 2005. The global effects of impact-induced seismic activity on fractured asteroid surface morphology. *Icarus* 179, 325–349. doi:[10.1016/j.icarus.2005.07.005](https://doi.org/10.1016/j.icarus.2005.07.005).
- Rivkin, A.S., Binzel, R.P., Sunshine, J., Bus, S.J., Burbine, T.H., Saxena, A., 2004. Infrared spectroscopic observations of 69230 Hermes (1937 UB): possible unweathered endmember among ordinary chondrite analogs. *Icarus* 172, 408–414. doi:[10.1016/j.icarus.2004.07.006](https://doi.org/10.1016/j.icarus.2004.07.006).
- Rivkin, A.S., Thomas, C.A., Trilling, D.E., Enga, M.T., Grier, J.A., 2011. Ordinary chondrite-like colors in small Koronis family members. *Icarus* 211, 1294–1297. doi:[10.1016/j.icarus.2010.11.033](https://doi.org/10.1016/j.icarus.2010.11.033).
- Roberts, L.C., Hall, D.T., Lambert, J.V., Africano, J.L., Knox, K.T., Barros, J.K., Hamada, K.M., Liang, D., Sydney, P.F., Kervin, P.W., 2007. Characterization of the near-Earth Asteroid 2002 NY₄₀. *Icarus* 192, 469–474. doi:[10.1016/j.icarus.2007.08.007](https://doi.org/10.1016/j.icarus.2007.08.007), [arXiv:0709.0984](https://arxiv.org/abs/0709.0984).
- Roush, T.L., 1984. Effects of temperature on remotely sensed mafic mineral absorption features. Master’s thesis. University of Hawaii.
- Rubincam, D.P., 2000. Radiative Spin-up and Spin-down of Small Asteroids. *Icarus* 148, 2–11. doi:[10.1006/icar.2000.6485](https://doi.org/10.1006/icar.2000.6485).
- Sanchez, J.A., Michelsen, R., Reddy, V., Nathues, A., 2013. Surface composition and taxonomic classification of a group of near-Earth and Mars-crossing asteroids. *Icarus* 225, 131–140. doi:[10.1016/j.icarus.2013.02.036](https://doi.org/10.1016/j.icarus.2013.02.036), [arXiv:1302.4449](https://arxiv.org/abs/1302.4449).
- Sanchez, J.A., Reddy, V., Nathues, A., Cloutis, E.A., Mann, P., Hiesinger, H., 2012. Phase reddening on near-Earth asteroids: Implications for mineralogical analysis, space weathering and taxonomic classification. *Icarus* 220, 36–50. doi:[10.1016/j.icarus.2012.04.008](https://doi.org/10.1016/j.icarus.2012.04.008), [arXiv:1205.0248](https://arxiv.org/abs/1205.0248).
- Shestopalov, D.I., Golubeva, L.F., Cloutis, E.A., 2013. Optical maturation of asteroid surfaces. *Icarus* 225, 781–793. doi:[10.1016/j.icarus.2013.05.002](https://doi.org/10.1016/j.icarus.2013.05.002).
- Shkuratov, Y., Starukhina, L., Hoffmann, H., Arnold, G., 1999. A Model of Spectral Albedo of Particulate Surfaces: Implications for Optical Properties of the Moon. *Icarus* 137, 235–246. doi:[10.1006/icar.1998.6035](https://doi.org/10.1006/icar.1998.6035).
- Sunshine, J.M., Bus, S.J., Corrigan, C.M., McCoy, T.J., Burbine, T.H., 2007. Olivine-dominated asteroids and meteorites: Distinguishing nebular and igneous histories. *Meteoritics and Planetary Science* 42, 155–170. doi:[10.1111/j.1945-5100.2007.tb00224.x](https://doi.org/10.1111/j.1945-5100.2007.tb00224.x).
- Thomas, C.A., Emery, J.P., Trilling, D.E., Delbó, M., Hora, J.L., Mueller, M., 2014. Physical characterization of Warm Spitzer-observed near-Earth objects. *Icarus* 228, 217–246. doi:[10.1016/j.icarus.2013.10.004](https://doi.org/10.1016/j.icarus.2013.10.004), [arXiv:1310.2000](https://arxiv.org/abs/1310.2000).
- Thomas, C.A., Rivkin, A.S., Trilling, D.E., Marie-Therese Enga, Grier, J.A., 2011. Space weathering of small Koronis family members. *Icarus* 212, 158–166. doi:[10.1016/j.icarus.2010.12.021](https://doi.org/10.1016/j.icarus.2010.12.021).
- Thomas, C.A., Trilling, D.E., Rivkin, A.S., 2012. Space weathering of small Koronis family asteroids in the SDSS Moving Object Catalog. *Icarus* 219, 505–507. doi:[10.1016/j.icarus.2012.01.020](https://doi.org/10.1016/j.icarus.2012.01.020).
- Vernazza, P., Binzel, R.P., Rossi, A., Fulchignoni, M., Birlan, M., 2009. Solar wind as the origin of rapid reddening of asteroid surfaces. *Nature* 458, 993–995. doi:[10.1038/nature07956](https://doi.org/10.1038/nature07956).
- Vernazza, P., Binzel, R.P., Thomas, C.A., DeMeo, F.E., Bus, S.J., Rivkin, A.S., Tokunaga, A.T., 2008. Compositional differences between meteorites and near-Earth asteroids. *Nature* 454, 858–860. doi:[10.1038/nature07154](https://doi.org/10.1038/nature07154).
- Vernazza, P., Marsset, M., Beck, P., Binzel, R.P., Birlan, M., Cloutis, E.A., DeMeo, F.E., Dumas, C., Hiroi, T., 2016. Compositional Homogeneity of CM Parent Bodies. *Astronomical Journal* 152, 54. doi:[10.3847/0004-6256/152/3/54](https://doi.org/10.3847/0004-6256/152/3/54).
- Walsh, K.J., Richardson, D.C., Michel, P., 2008. Rotational breakup as the origin of small binary asteroids. *Nature* 454, 188–191. doi:[10.1038/nature07078](https://doi.org/10.1038/nature07078).
- Warner, B.D., Harris, A.W., Pravec, P., 2009. The asteroid lightcurve database. *Icarus* 202, 134–146. doi:[10.1016/j.icarus.2009.02.003](https://doi.org/10.1016/j.icarus.2009.02.003).
- Wetherill, G.W., 1967. Collisions in the Asteroid Belt. *Journal of Geophysical Research* 72, 2429. doi:[10.1029/JZ072i009p02429](https://doi.org/10.1029/JZ072i009p02429).
- Whiteley, Robert Jennings, J., 2001. A compositional and dynamical survey of the near-Earth asteroids. Ph.D. thesis. University of Hawai’i at Manoa.
- Wisniewski, W.Z., 1991. Physical studies of small asteroids and cometary nuclei. In NASA, Washington, Reports of Planetary Astronomy, 1991 p 135-136 (SEE N92-12792 03-89).